ISSN.: 2349-7866

Fabrication of Cost Effective Highly Sensitive Gas Sensing Films Deposited Using a Simple Automated Nebulizer Spray Technique

A. Manivasaham[1]
[1]Assistant Professor, Department of Science and Humanities (Physics), M. Kumarasamy College of Engineering, Karur, Tamil Nadu, India. Email: maanivasahham@gmail.com

Abstract: The automated jet nebulizer spray pyrolysis technique was exploiting to deposit ZnO thin films over the glass substrates maintained at temperature 300^{0}C. The effect of volume of the precursor solution over the structural, surface morphological, compositional, optical, electrical and gas sensing properties of ZnO thin films were studied. X-ray diffraction results show that the deposited films are having hexagonal structure with (002) as high preferential orientation plane. SEM studies shows uniformly distributed hexagonal shaped crystals over the surface. Photoluminescence band edge emission at 384 nm, indicates the high crystal quality. From the optical measurements, it is found that the prepared films have a maximum transmittance greater than 90% and direct band gap energy below 3.36 eV. The gas sensing characteristics of the fabricated material was studied by exposing it to ammonia gas. The gas sensitivity, response time and recovery time are studied and reported.

Keywords: Ammonia sensor, Automated jet nebulizer, ZnO.

I. Introduction

In order to control and monitor air pollution, novel ideas toward the design and development of simple and inexpensive semiconductor oxide gas sensors have to be implemented. Among the various deadly gases, ammonia can cause several problems to human respiratory system and skin [1,2]. The acceptable exposure limit of ammonia is only 25 ppm for long-term (8h) and 35 ppm for short-term (15 min) as reported by Occupational Safety and Health Administration (OSHA) [3,4].

In recent years, researchers have focused on the development of microsensors which have both high sensitivity and selectivity for specific gases with cost effective on sensing [1,2].

Among various semiconductor oxide materials, ZnO is a tunable, flexible, abundantly available and low cost in fabrication [5]. Surface-to-volume ratios and high one-dimensional electron mobility along growth directions are very important property for gas sensing [6]. ZnO based thin films have several other advantages to have suitable and excellent control over morphology and position, high thermal stability, non-stoichiometry, and oxygen vacancies [7].

Various deposition techniques have been widely used to produce ZnO thin films like chemical bath deposition, RF magnetron sputtering, sol–gel method, chemical vapor deposition (CVD), thermal evaporation and spray pyrolysis [8-16]. As cost effective fabrication of ZnO based sensors is one of the major goals of this work, the nebulizer spray technique is adopted for the preparation of ZnO based gas sensors [17-21].

Surface morphology of ZnO changes with the change in thickness of the ZnO films and the effect of thickness on the structural, optical and electrical properties of ZnO thin films was investigated. Its adaptability towards application in the field of thin film gas sensors also investigated.

II. Thin Film Deposition

A fully automated jet nebulizer spray unit was used to fabricate ZnO thin films on to methodically cleaned glass substrates [22]. The deposition parameters are given in Table I.

Table I: Optimized Deposition Parameter for ZnO Thin Films

Parameter	Value
Nozzle diameter	10 mm
Spray rate	0.637 mL min−1
Pressure of Carrier gas	1.5 bar
Spray time	10 s
Successive sprays interval	10 s
Substrate – nozzle distance	10 cm
Substrate temperature	300^{0}C
Volume of precursor	15, 20 and 25mL

The precursor solution was prepared by dissolving 0.1 M of zinc acetate dihydrate ($Zn(CH_3COO)_2{\cdot}2H_2O$) in the mixture of doubly deionized water, methanol and acetic acid in the ratio 7:2:1. It has filled in reservoir and pressurized by double filtered oil / moisture free compressed air to get the uniform deposition on the glass substrate. The jet nebulizer spray unit can be moved horizontally for the area of 3 x 8 cm^2. Microscopic glass slides (Labtech medico (P) Ltd, Mumbai) were cleaned systematically with HCl, acetone and deionized water. Before cleaning substrates was placed in ultrasonic bath (Supersonics, Mumbai) for 30 min and dried in hot plate at 100°C for 20 min to remove organic substance and other moistures present if any on the substrate surface. The glass substrates were carefully positioned on the hot plate. To facilitate the reproducibility and performance characterization studies, all together 3 x 5 samples were prepared.

III. Thin Film Characterization

X-ray diffractometer (PAN alytical-PW 340/60 X' Pert PRO) with X-ray (Cu–Ka) of wavelength 1.5406 Å was used to study the structural properties of the films. Thickness of the films was measured by means of both stylus technique (profilometer: Surf Test SJ- 301) and weight gain method. The thickness was found to be in the range of 400, 600 and 800 nm for the sample A, B and C respectively. The UV-vis-NIR double beam spectrophotometer (LAMBDA-35) was used to study optical properties of the films in the wavelength range of 300-1100 nm. The electrical resistivity of the films was determined using four point probe technique with Vander Paw configuration. The SEM images were obtained by employing scanning electron microscope (HITACHI S-3000 H). The Photoluminescence (PL) studies were carried out using a spectro-flurometer (Jobin Yvon_FLUROLOG-FL3-11) with xenon lamp (450 W) as the source for the excitation wavelength of 325 nm. Gas sensing was made by using a homemade gas test chamber [23].

A. Gas Sensing Mechanism

Gas sensing properties of ZnO films were studied using a homemade gas test chamber made up of stainless steel. 2 L round bottom flask and cylinder containing pressured air are connected to the gas test chamber. Inside the chamber, a sample holder is used to clamp the sample and contacts were made with the help of silver paste which is applied on either sides of the sample and a thermocouple was placed to measure the inner temperature of the chamber. Sample holder was connected to a precession multimeter to measure the change in resistance during gas sensing process.

The chromatographic syringe are used inject solution of gas into the flask by. The volume of solution with respect to concentration (ppm) [24] was calculated from the equation (1).

$$C_{ppm} = \frac{\delta \times V_r \times R \times T}{M \times P_b \times V_b} \times 10^6 \quad (1)$$

where T, R, δ, V_r, M, P_b, and V_b are the absolute temperature, the universal gas constant the density of ammonia solution, the volume of ammonia injected, and (8.3145 J/mol K), the molecular weight of ammonia solution, pressure inside the chamber and volume of the chamber respectively.

The solution was injected and gets vaporized at room temperature and the total volume of the chamber is around 0.024m^3. When the ammonia gas enters into the chamber, the resistance of the sample starts decreasing and the change in resistance was recorded with respect to time. During the sensing process, when the sample resistance remains constant, air cylinder was opened to regain its air resistance. This process completes one cycle of sensing.

At room temperature, the gas sensing was made and the sensing area of all the films was kept constant as 2 cm^2.

The surface morphology determines the trapping and gas detection mechanism, the atmospheric oxygen are trapped on the surface porous, leads to increase in resistance. The applied gas removes the trapped oxygen from the surface and librates electrons to the surface and oxygen acquires electrons from the conduction band of ZnO, resulting in the formation of oxygen ions (O_2^-) represented by the equation [24].

$$O_2 + e^- \rightarrow O^-_{2(ads)}$$

Due to this formation of oxygen ions, the resistance of the ZnO film initially increases and reaches its saturation level which is denoted as "air resistance (R_a)". The resistance then decreases linearly with the increase the gas level of and attains a low value represented as "gas resistance (R_g)" for each concentration of ammonia gas tested.

The following equation represents the overall reducing reaction [25].

$$4NH_3 + O^-_{2(ads)} \rightarrow 2N_2 + 6\,H_2O + 6e^-$$

The released free electrons will increase the carrier concentration and as a result, the resistance decreases to a minimum value, denoted as R_g. This R_g varies with variation in the concentration of the ammonia gas. The resistances R_a and R_g are noted at interval of 20 sec repeatedly.

IV. Results and Discussion

A. Optical and Electrical Properties

The optical transmittance spectra of ZnO thin films deposited at three different thickness (400, 600 and 800 nm) are shown in Fig. 1(a). The average transmittance in the visible region is around 90% for the sample A. The transmittance increases with

the increase in thickness of the film and reaches a maximum value of 92% for the film having thickness 800 nm [25]. The increase in transmittance may be attributed to the increase in grain size as observed from the FESEM images (Section D).

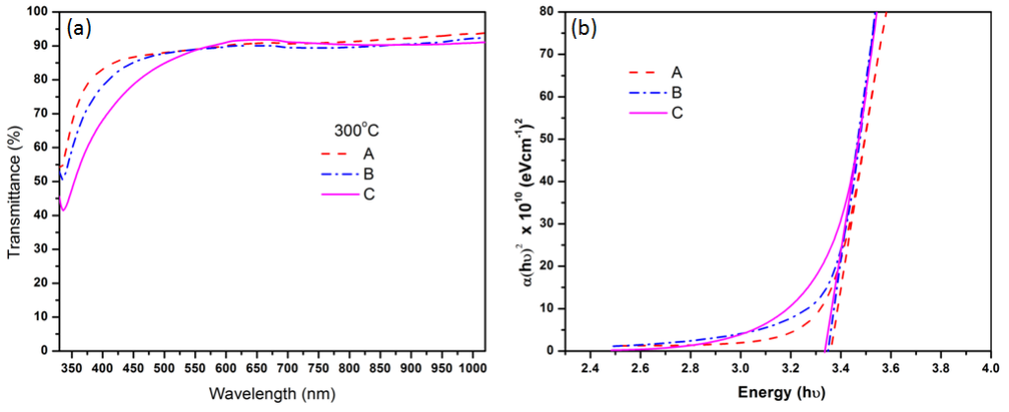

(a) (b)

Fig. 1: (a) Transmittance Spectra and (b) Tauc's Plot of all the Deposited Films

From the Tauc's plots shown in Fig. 1(b) [27], the band gap values are 3.36, 3.35 and 3.33 for the samples A, B and C respectively. It is found that there is a marginal decrease in the E_g value with the increase in the thickness of the sample. This may be due to the increase in the carrier concentration according to the Moss–Burstein effect [27,28].

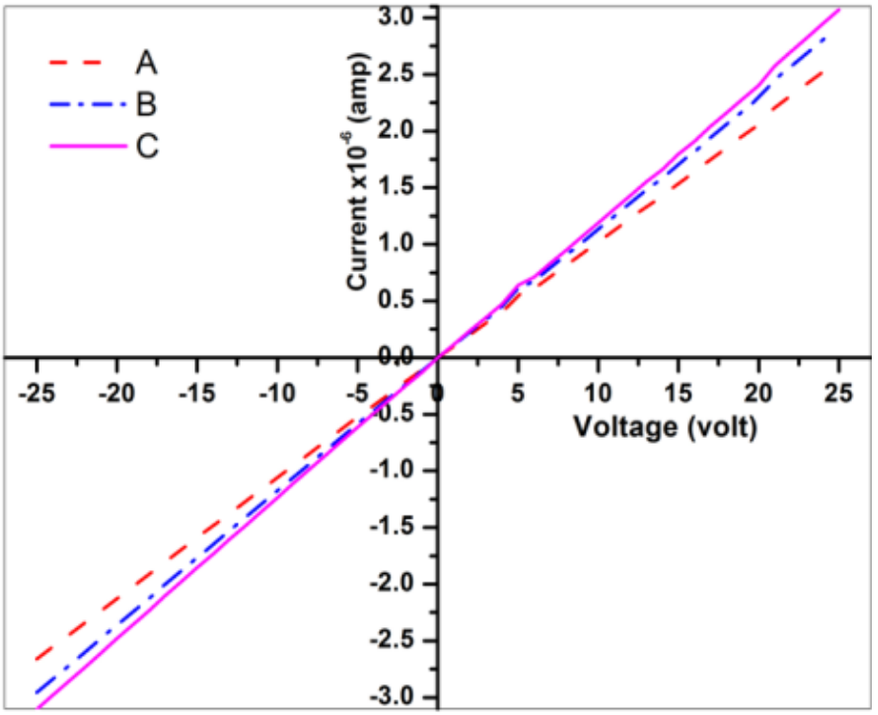

Fig. 2: Voltage Current Characteristics of the ZnO Films

The voltage current characteristics of all the deposited samples are shown in Fig. 2. The output current increases linearly with respect to the input voltage in all cases. The ZnO films act like a resistor and obey Ohm's law (V=IR) as obvious from the plots. From the graph it is observed that the current increases as the thickness increases and also it was confirmed that the ohmic contacts were well established.

B. Photo Luminescence Studies

The PL spectra of the ZnO thin films are shown in Fig. 3. The Near Band Edge (NBE) emission for the samples occurs at about 384 nm [29]. It is seen from Fig. 3 that the NBE peak slightly shifts towards right with the increase of thickness. Generally, shift in NBE peak occurs when there is a change in band gap.

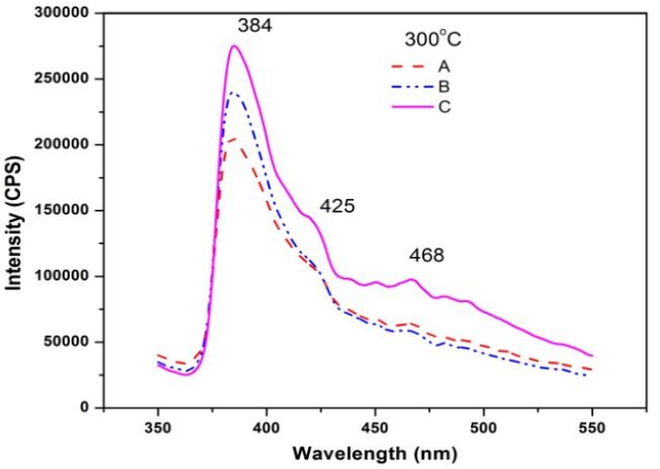

Fig. 3: PL Spectra of the Films Deposited with Three Different Thickness

This result is in consistent with the optical band gap values estimated from the Tauc's plots (Section A). The peaks around 425 and 468 nm are corresponding to defect level emissions related to the zinc interstitials and singly ionized oxygen vacancies, respectively [30-32]. It is found that among all the samples, the sample C having thickness about 800 nm has higher number of singly ionized oxygen vacancies and attract more NH_3 gas molecules than other two samples.

C. Structural Studies

The XRD patterns of ZnO thin films are shown in Fig. 4(a). All the observed peaks are matched well with the JCPDS data card no. 36-1451 [33]. This result confirms that all the prepared samples are having single phase with polycrystalline hexagonal wurtzite structure of ZnO. Hence, it is concluded that the variation of thickness does not alter the crystallographic structure of ZnO. However, as the thickness increases, the intensity of the peak (002) decreases gradually and intensity of the peak (101) increases indicating a gradual improvement in the crystalline quality of the films. It is observed from the Fig. 4(b) that, the intensity of the (002) peak is maximum and which implies that the grains are prefer to grow along the c-axis.

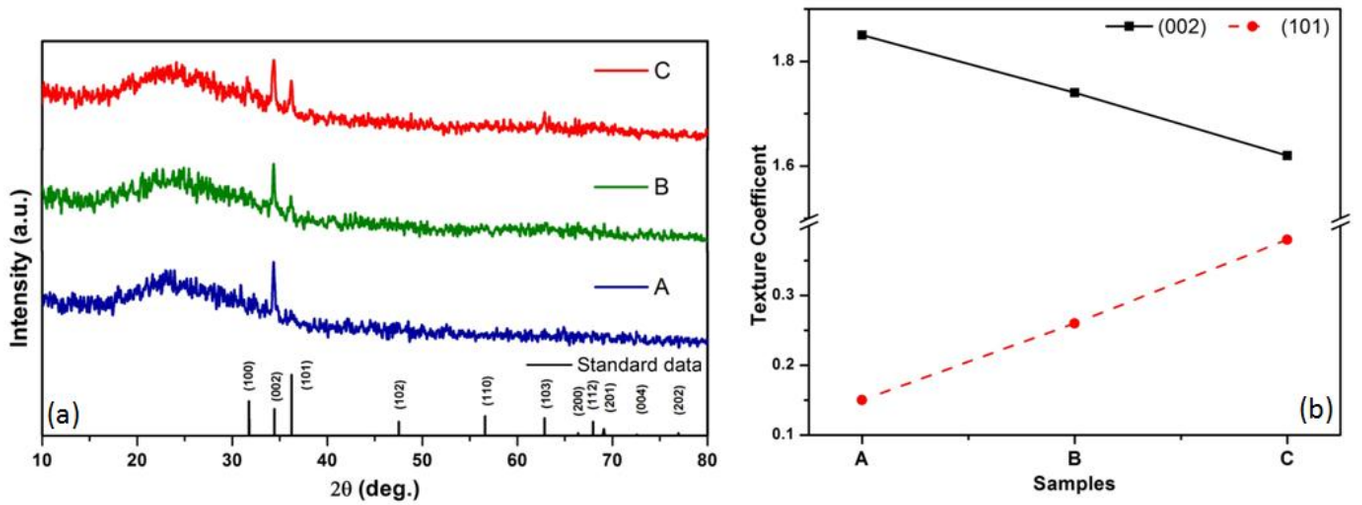

(a) (b)

Fig. 4: (a) X-ray Diffraction Patterns of the ZnO films (b) Texture Coefficient of Three Different Thicknesses of ZnO Samples for the Planes (002) and (101)

The crystallite size (D) of the films is estimated using the Scherrer's formula [34] $D = 0.9\lambda / (\beta \cos\theta)$ where λ is the wavelength of the X-ray used (1.5406 Å), β is the full-width at half-maximum intensity (FWHM) and θ is the angle of diffraction. From the calculated 'D' values, it is found that, samples A, B and C have the crystallite size around 14, 30 and 52 nm, respectively. This result is agreed well with the grain size observed from the FESEM images.

D. Surface Morphological and Compositional Studies

The surface morphological images of all the three samples are shown in Fig. 5 (a-c). Fig. 5 shows the grains having defined boundaries present on the surface of all the films and the grain size of A sample is lesser as that of other two samples. The decrease of grain size able to increase the surface to volume ratio of samples. The inset table shows the atomic proportions of the constituent elements.

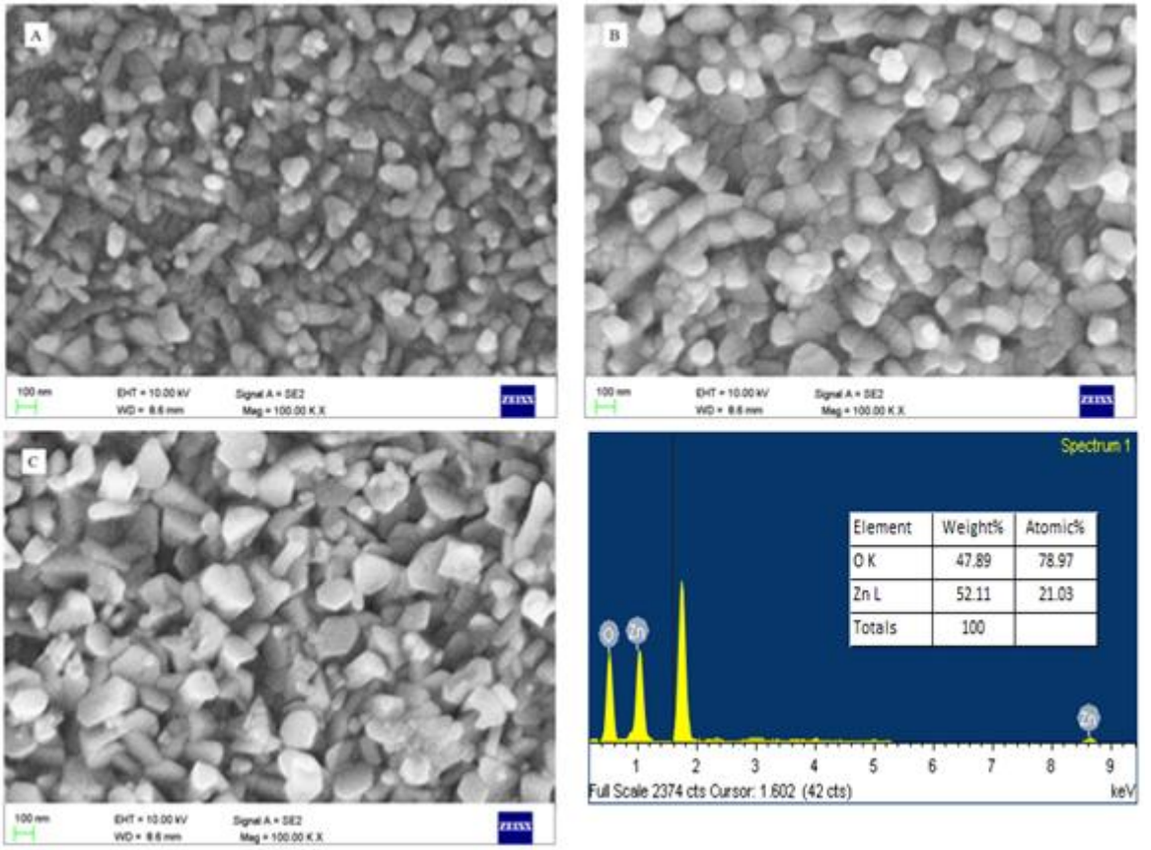

Fig. 5: (a-c) FESEM Images of the Films Having Three Different Thickness and (d) EDAX Spectrum of the ZnO Film with the Thickness 800 nm

As size of grains are smaller, leads to increases effective sensing area and thereby increases the gas sensing property of the samples. It is seen from the figure that, the surface of sample C consists of relatively large porosity than that of other two samples which is the required main factor in order to attract and traps more number of oxygen on the surface. For better sensing ability, larger surface to volume ratio and surface porous are essential factors. In spite of the larger surface grains, the porous nature of sample C helps to achieve better sensing ability. Hence, it is concluded that, the large porous nature make this sample to have enhanced sensing ability when compared to the other two cases.

The EDAX image of the ZnO film (thickness 800 nm) is shown in Fig. 5(d). The image confirms the existence of the anticipated elements Zn and O in the sample. The atomic proportions of the constituent elements, zinc and oxygen are given in a Table as an inset of Fig. 5(d). This result showing the lesser atomic percentage of oxygen supports the discussion on the presence of oxygen vacancies in Section B.

E. Gas Sensing Study

Sample is fixed on the substrate holder and the air resistance is recorded (R_a), then 10 ppm gas was injected into the flask. The variation in resistance is recorded continuously with respect to

time. Resistance is recorded until it reaches a constant resistance R_g and dry air was allowed to regain R_a. Gas sensing process was experimented for different gas concentration levels *viz.*10, 20, 40, 60, 80, 100, 200 and 300 ppm.

The observed cyclic response of all three samples is shown in Fig. 6 (a-c). The recovery times and response are calculated using the equations (2) and (3) [22].

$$\text{Response time } (t_{Res}) = (t_{Ra} \sim t_{Rg}) \text{ x } 90/100 \quad (2)$$

$$\text{Recovery time } (t_{Rec}) = (t_{Ra} \sim t_{Rg}) \text{ x } 10/100 \quad (3)$$

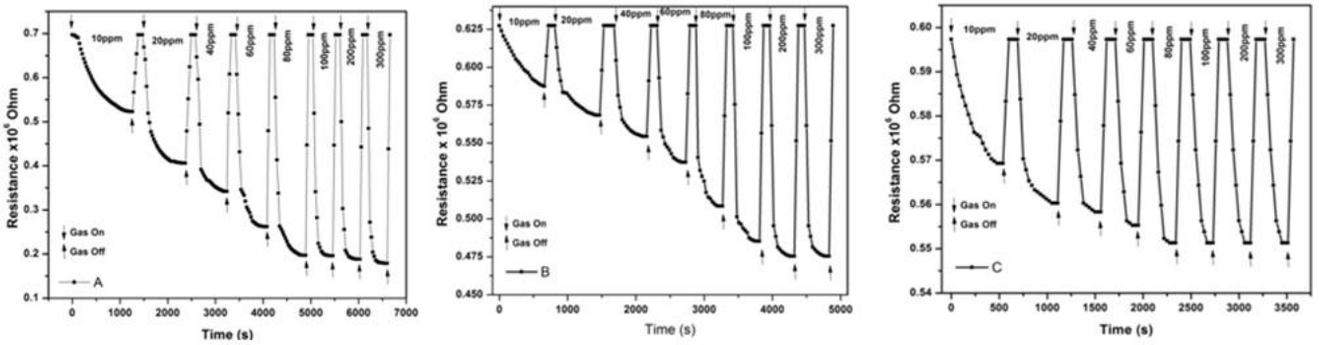

Fig. 6: (a-c) Variation in Resistance w.r.t. Time for Different Gas Concentrations

Fig. 6 shows the response and recovery times of all the samples. It is observed from the table that, the sample C has lesser response time than other two samples for all the tested concentration of the ammonia gas. It is also observed that for higher order concentration of gas i.e. more than 100 ppm, response time remains same. This is due to the decrease of active site, present on the surface of the sample and the response time of all the samples decreases when the concentration of ammonia gas increases (Fig. 6(a)). This decreasing trend is owing to the interaction of higher number of ammonia molecules with the surface of the films.

In general, the recovery time of any sensing element is lesser than response time [37]. The grain size, number of oxygen vacancies and surface morphology are the deciding factors for the efficiency of a sensing element. In the present work also, the recovery time is shorter than the response time which may be due to the quick reaction rate between the film surface and dry air. This is because of the fact that the film surface adsorbs oxygen to compensate the native deficiency of oxygen. The higher deficiency of oxygen in the sample C (thickness 800 nm) is confirmed by the PL results. Generally spray pyrolysis technique creates large deficiency in oxygen in the deposited films [38].

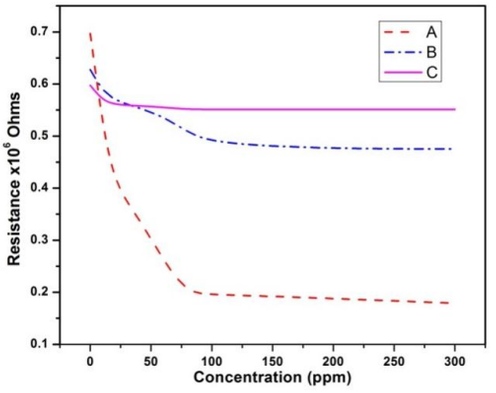

Fig. 7: Plots of Resistance Variation Vs Gas Concentration

From the Fig. 7 the resistance R_g of sample A decreases gradually upto 100 ppm and thereafter (100 ppm to 300 ppm), R_g decreases marginally [39]. This is due to the small grain size for sample A. For sample B and C, the resistance decreases uniformly with respect to gas concentration which may be due to the surface morphological changes. Moreover, during recovery process, large number of oxygen molecules adsorbed by the film surface is the main factor to regain its air resistance [39].

V. Conclusion

ZnO thin films with three different thicknesses (400, 600 and 800 nm) were coated uniformly on glass substrates at a substrate temperature of 300°C using an automated jet nebulizer spray. The sensing ability of deposited films were tested for different concentrations of ammonia gas *viz.* 10, 20, 40, 60, 80, 100, 200 and 300 ppm under darkness. The sample with the thickness of 800 nm (sample C) shows better sensing ability than other two samples. This enhanced sensitivity of this sample may be due to the increased effective interactive area and larger number of pores of this film as evident from the surface morphological studies. The presence of large number of oxygen vacancies in this sample as evidenced by the PL studies supports the above inference. Even though the other two samples have a better surface to volume ratio than sample C, presence of lesser number of pores on the surface and the lesser number of oxygen vacancies in these samples resulting in lesser sensing ability than sample C. Hence, 800 nm is the best suited film thickness for ZnO film for sensing ammonia gas.

Reference

[1] K. Wetchakun, T. Samerjai, N. Tamaekong, C. Liewhiran, C. Siriwong, V. Kruefu, A. Wisitsoraat, A. Tuantranont, and S. Phanichphant, "Semiconductor metal oxides as sensor for environmentally hazardous

gases," *Sens. Actuators B: Chem,* vol. 160, pp. 580-591, 2011.

[2] Y.-F. Sun, S.-B. Liu, F.-L. Meng, J.-Y. Liu, Z. Jin, J.-H. Liu, and L.-T. Kong, "Metal oxide nanostructures and their gas sensing properties: A review," *Sensors,* vol. 12, no. 3, pp. 2610-2631, 2012.

[3] A. K. Radzimska, and T. Jesionowski, "Zinc oxide-from synthesis to application: A review," *Materials,* vol. 7, no. 4, pp. 2833-2881, 2014.

[4] U. Özgür, Y. I. Alivov, C. Liu, A. Teke, M. A. Reshchikov, S. Do˘gan, V. Avrutin, S.-J. Cho, and H. Morkoç, "A comprehensive review of ZnO materials and devices," *Journal of Applied Physics,* vol. 98, no. 4, 2005.

[5] T. P. Rao, M. C. S. Kumar, A. Safarulla, V. Ganesan, S. R. Barman, and C. Sanjeeviraja, "Physical properties of ZnO thin films deposited at various substrate temperatures using spray pyrolysis," *Physica B: Condensed Matter*, vol. 405, no. 9, pp. 2226-2231, 2010.

[6] C. Shao, Y. Chang, and Y. Long, "High performance of nanostructured ZnO film gas sensor at room temperature," *Sensors and Actuators B: Chemical*, vol. 204, pp. 666-672, 2014.

[7] G. K. Mani, and J. B. B. Rayappan, "Novel and facile synthesis of randomly interconnected ZnO nanoplatelets using spray pyrolysis and their room temperature sensing characteristics," *Sensors and Actuators B: Chemical*, vol. 198, pp. 125-133, 2014.

[8] C. Cachoncinlle, C. Hebert, J. Perriere, M. Nistor, A. Petit, and E. Millon, "Random lasing of ZnO thin films grown by pulsed-laser deposition," *Applied Surface Science,* vol. 336, pp. 103-107, 2015.

[9] F.-H. Wang, and C.-L. Chang, "Effect of substrate temperature on transparent conducting Al and F codoped ZnO thin films prepared by rf magnetron sputtering," *Applied Surface Science,* vol. 370, pp. 83-91, 2016.

[10] R. Mariappan, V. Ponnuswamy, P. Suresh, N. Ashok, P. Jayamurugan, and A. C. Bose, "Influence of film thickness on the properties of sprayed ZnO thin films for gas sensor applications," *Superlattices and Microstructures*, vol. 71, pp. 238-249, 2014.

[11] H. Xia, T. Liu, L. Gao, L. Yan, and J. Wu, "Development of film sensors based on ZnO nanoparticles for amine gas detection," *Applied Surface Science*, vol. 258, no. 1, pp. 254-259, 2011.

[12] A. P. Ramu, D. Sirbu, N. Iftimie, and G. I. Rusu, "Polycrystalline ZnO-In_2O_3 thin films as gas sensors," *Thin Solid Films*, vol. 520, no. 4, pp. 1303-1307, 2011.

[13] B. Renganathan, D. Sastikumar, G. Gobi, N. R. Yogamalar, and A. C. Bose, "Nanocrystalline ZnO coated fiber optic sensor for ammonia gas detection," *Optics & Laser Technology,* vol. 43, no. 8, pp. 1398-1404, 2011.

[14] B. Timmer, W. Olthuis, and A. Van Den Berg, "Ammonia sensors and their applications - A review," *Sensors and Actuators B: Chemical*, vol. 107, no. 2, pp. 666-677, 2005.

[15] C. Jing, and W. Tang, "Ga-doped ZnO thin film surface characterization by wavelet and fractal analysis," *Applied Surface Science,* vol. 364, pp. 843-866, 2016.

[16] K. Ravichandran, P. Sathish, B. Muralidharan, B. Sakthivel, K. Swaminathan, A. Panneerselvam, and G. Muruganandam, "Influence of a novel triple doping (Ag+Mn+F) on the magnetic and antibacterial properties of ZnO nanopowders," *Ceramics International*, vol. 42, no. 2 part A, pp. 2349-2356, 2016.

[17] R. Mariappan, V. Ponnuswamy, R. Suresh, P. Suresh, A. C. Bose, and M. Ragavendar, "Role of substrate temperature on the properties of Na-doped ZnO thin film nanorods and performance of ammonia gas sensors using nebulizer spray pyrolysis technique," *Journal of Alloys and Compounds*, vol. 582, pp. 387-391, 2014.

[18] C. Ravidhas, B. Anitha, A. M. E. Raj, K. Ravichandran, T. C. S. Girisun, K. Mahalakshmi, K. Saravanakumar, and C. Sanjeeviraja, "Effect of nitrogen doped titanium dioxide (N-TiO_2) thin films by jet nebulizer spray technique suitable for photoconductive study," *Journal of Materials Science Materials in Electronics,* 2015.

[19] A. Mahroug, S. Boudjadar, S. Hamrit, and L. Guerbous, "Structural, optical and photocurrent properties of undoped and Al-doped ZnO thin films deposited by sol–gel spin coating technique," *Materials Letters*, vol. 134, pp. 248-251, 2014.

[20] V. Senthamilselvi, K. Ravichandran, and K. Saravanakumar, "Influence of immersion cycles on the stoichiometry of CdS films deposited by SILAR technique," *Journal of Physics and Chemistry of Solids*, vol. 74, no. 1, pp. 65-69, 2013.

[21] O. Lupan, T. Pauporté, I. M. Tiginyanu, V. V. Ursaki, V. Şontea, L. K. Ono, B. R. Cuenya, and L. Chow, "Comparative study of hydrothermal treatment and thermal annealing effects on the properties of electrodeposited micro-columnar ZnO thin films," *Thin Solid Films*, vol. 519, pp. 7738-7749, 2011.

[22] I. Muniyandi, G. K. Mani, P. Shankar, and J. B. B. Rayappann, "Effect of nickel doping on structural, optical, electrical and ethanol sensing properties of spray deposited nanostructured ZnO thin films," *Ceramics International*, vol. 40, no. 6, pp. 7993-8001, 2014.

[23] B. Poornaprakash, D. A. Reddy, G. Murali, N. M. Rao, R. P. Vijayalakshmi, and B. K. Reddy, "Composition dependent room temperature ferromagnetism and PL intensity of cobalt doped ZnS nanoparticles," *Journal of Alloys and Compounds*, vol. 577, pp. 79-85, 2013.

[24] Z. Yang, Y. Huang, G. Chen, Z. Guo, S. Cheng, and S. Huang, "Ethanol gas sensor based on Al-doped ZnO nanomaterial with many gas diffusing channels," *Sensors and Actuators B: Chemical*, vol. 140, no. 2, pp. 549-556, 2009.

[25] S. Snega, K. Ravichandran, M. Baneto, and S. Vijayakumar, "Simultaneous enhancement of transparent and antibacterial properties of ZnO films by suitable F doping," *Journal of Materials Science & Technology*, vol. 31, pp. 759-765, 2015.

[26] R. Anandhi, R. Mohan, K. Swaminathan, and K. Ravichandran, "Influence of aging time of the starting solution on the physical properties of fluorine doped zinc oxide films deposited by a simplified spray pyrolysis technique," *Superlattices and Microstructures*, vol. 51, no. 5, pp. 680-689, 2012.

[27] G. Muruganantham, K. Ravichandran, K. Saravanakumar, A. T. Ravichandran, and B. Sakthivel, "Effect of solvent volume on the physical properties of undoped and fluorine doped tin oxide films deposited using a low-cost spray technique," *Superlattices and Microstructures,* vol. 50, no. 6, pp. 722-733, 2011.

[28] K. Ravichandran, P. Sathish, B. Muralidharan, B. Sakthivel, K. Swaminathan, A. Panneerselvam, and G. Muruganandam, "Influence of a novel triple doping (Ag+Mn+F) on the magnetic and antibacterial properties of ZnO nanopowders," *Ceramics International*, vol. 42, no. 2 part A, pp. 2349-2356, 2016.

[29] K. Ravichandran, R. Mohan, N. J. Begum, S. Snega, K. Swaminathan, C. Ravidhas, B. Sakthivel, and S. Varadharajaperumal, "Impact of spray flux density and vacuum annealing on the transparent conducting properties of doubly doped (Sn + F) zinc oxide films deposited using a simplified spray technique," *Vacuum*, vol. 107, pp. 68-76, 2014.

[30] I. A. Pronin, D. T. Dimitrov, L. K. Krasteva, K. I. Papazova, I. A. Averin, A. S. Chanachev, A. S. Bojinova, A. T. Georgieva, N. D. Yakushova, and V. A. Moshnikov, "Theoretical and experimental investigations of ethanol vapour sensitive properties of junctions composed from produced by sol–gel technology pure and Fe modified nanostructured ZnO thin films," *Sensors and Actuators A: Physical*, vol. 206, pp. 88-96, 2014.

[31] X. Du, and S. M. George, "Thickness dependence of sensor response for CO gas sensing by tin oxide films grown using atomic layer deposition," *Sensors and Actuators B: Chemical*, vol. 135, no. 1, pp. 152-160, 2008.

[32] K. L. A. Kumar, S. Durgajanani, B. G. Jeyaprakash, and J. B. B. Rayappan, "Nanostructured ceria thin film for ethanol and trimethylamine sensing," *Sensors and Actuators B: Chemical*, vol. 177, pp. 19-26, 2013.

[33] Z. Pan, Y. Xiao, X. Tian, S. Wu, C. Chen, J. Deng, C. Xiao, G. Hu, and Z. Wei, "Effect of annealing on the structures and properties of Al and F co-doped ZnO nanostructures," *Materials Science in Semiconductor Processing*, vol. 17, pp. 162-167, 2014.

[34] K. Ravichandran, K. Subha, N. Dineshbabu, and A. Manivasaham, "Enhancing the electrical parameters of ZnO films deposited using a low-cost chemical spray technique through Ta doping," *Journal of Alloys and Compounds*, vol. 656, pp. 332-338, 2016.

[35] V. K. Jayaraman, A. M. Álvarez, and M. L. O. Amador, "A simple and cost-effective zinc oxide thin film sensor for propane gas detection," *Materials Letters*, vol. 157, pp. 169-171, 2015.

[36] S.-S. Park, H. Zheng, and J. D. Mackenzie, "Ethanol gas sensing properties of SnO_2- based thin-film sensors prepared by the sol-gel process," *Materials Letters*, vol. 17, no. 6, pp. 346-352, 1993.

[37] S. H. Yan, S. Y. Ma, W. Q. Li, X. L. Xu, L. Cheng, H. S. Song, and X. Y. Liang, "Synthesis of SnO_2-ZnO heterostructured nanofibers for enhanced ethanol gas-sensing performance," *Sensors and Actuators B: Chemical*, vol. 221, pp. 88-95, 2015.

[38] S. Pati, P. Banerji, and S. B. Majumder, "Properties of indium doped nanocrystalline ZnO thin films and their enhanced gas sensing performance," *RSC Advances*, vol. 5, pp. 61230-61238, 2015.

[39] S. K. Shaikh, V. V. Ganbavle, S. I. Inamdar, and K. Y. Rajpure, "Multifunctional zinc oxide thin films for high-performance UV photodetectors and nitrogen dioxide gas sensors," *RSC Advances*, vol. 6, pp. 25641-25650, 2016.